Biogeochemistry (2013) 112:179–195
DOI 10.1007/s10533-012-9715-2

The influence of goethite and gibbsite on soluble nutrient dynamics and microbial community composition

Katherine Heckman · Amy Welty-Bernard · Angelica Vazquez-Ortega · Egbert Schwartz · Jon Chorover · Craig Rasmussen

Received: 19 May 2011 / Accepted: 12 February 2012 / Published online: 11 March 2012

Abstract Iron and aluminum (oxyhydr)oxides are ubiquitous in the soil environment and have the potential to strongly affect the properties of dissolved organic matter. We examined the effect of oxide surfaces on soluble nutrient dynamics and microbial community composition using an incubation of forest floor material in the presence of (1) goethite and quartz, (2) gibbsite and quartz, and (3) quartz surfaces. Forest floor material was incubated over a period of 154 days. Aqueous extracts of the incubations were harvested on days 5, 10, 20, 30, 60, 90, and 154, and concentrations of P, N, PO_4^{3-}, NO_2^-, NO_3^-, and organic C were measured in the solutions. Microbial community composition was examined through pyrosequencing of bacterial and fungal small subunit ribosomal RNA genes on selected dates throughout the incubation. Results indicated that oxide surfaces exerted strong control on soluble nutrient dynamics and on the composition of the decomposer microbial community, while possibly having a small impact on system-level respiration. Goethite and gibbsite surfaces showed preferential adsorption of P-containing and high molar mass organic solutes, but not of N-containing compounds. On average, organic C concentrations were significantly lower in water extractable organic matter (WEOM) solutions from oxide treatments than from the control treatment ($P = 0.0037$). Microbial community composition varied both among treatments and with increasing time of incubation. Variation in bacterial and fungal community composition exhibited strong-to-moderate correlation with length of incubation, and several WEOM physiochemical characteristics including apparent (weight averaged) molar mass, pH and electrical conductivity. Additionally, variation in bacterial community composition among treatments was correlated with total P ($r = 0.60$, $P < 0.0001$), PO_4^{3-} ($r = 0.79$, $P < 0.0001$), and organic C ($r = 0.36$, $P = 0.015$) concentrations; while variation in fungal communities was correlated with organic C concentrations ($r = -0.48$, $P = 0.0008$) but not with phosphorus concentrations. The relatively small impact of oxide surfaces on system-level microbial respiration of organic matter despite their significant effects on microbial community composition and WEOM dynamics lends additional support to the theory of microbial functional redundancy.

Keywords Water extractable organic matter · Goethite · Gibbsite · Soil microbial community composition · Forest floor · Forest C cycle

K. Heckman (✉) · A. Vazquez-Ortega · J. Chorover · C. Rasmussen
Department of Soil, Water & Environmental Science, University of Arizona, P.O. Box 210038, Tucson, AZ 85721-0038, USA
e-mail: kaheckman@fs.fed.us

A. Welty-Bernard · E. Schwartz
Department of Biological Sciences, Northern Arizona University, P.O. Box 5640, Flagstaff, AZ 86011-5640, USA

Introduction

Concerns over global climate change have increased interest in clarifying the mechanisms regulating organic C storage in soils. Forest soils contain a substantial portion of the world's C stocks, and therefore mechanisms regulating the size and turnover rate of organic matter in forest soils are of particular importance. Though dissolved organic matter (DOM) comprises only ~1% of the total organic C in soils, DOM is the most mobile fraction of soil organic carbon (Zsolnay 1996) and is a significant source of new C inputs to subsurface soils in temperate forest systems (Zech and Guggenberger 1996). Previous research has also suggested that biodegradation of soil organic matter occurs dominantly in the aqueous phase (Kalbitz et al. 2003) and that DOM may be the most important C source for soil microbes (Metting 1993; Jandl and Sollins 1997; Wagai and Sollins 2002; Marschner and Kalbitz 2003). Therefore, changes in the composition and solid-solution partitioning of DOM and associated inorganic solutes may have a profound influence on C mineralization rates and both the size and activity of the microbial decomposer community.

Much work has focused on organo-mineral interactions in soil (e.g. Lützow et al. 2006; Kögel-Knabner et al. 2008), but a substantial knowledge gap remains concerning the complex interactions among soil mineral, organic, and microbial components (Six et al. 2002; Mikutta et al. 2006; Schmidt et al. 2011). This is especially true in regards to how these interactions change throughout the biodegradation process (Grandy et al. 2007; Grandy and Neff 2008). General examinations of the biogeochemistry of SOM degradation in natural soils have indicated that mineral, biological, and organic components of soil influence one another in complex and multifaceted ways. In addition, the important influence of the mineral matrix on the biodegradation process has been highlighted by recent work. However, investigation into organo-mineral-microbe relationships in the soil environment is significantly hampered by the implicit complexity of natural soils. The current study was designed to examine the dynamic interactions among dissolved organics, microbial communities, and mineral surfaces, and how the relationships among these components change with increasing degree of organic matter decomposition. Using simplified systems under controlled conditions reduced the number of confounding factors influencing mineral-microbe-SOM interactions, and allowed for more quantitative measurement of these interactions than would be possible if natural soils were used.

Sorption of organic matter to mineral surfaces has been recognized as one of the most important stabilization mechanisms controlling organic C content in sediments and soils (Keil et al. 1994; Kalbitz et al. 2003; Kögel-Knabner et al. 2008; among others). Sorption has been shown to reduce the bioavailability of microbial substrates and can greatly reduce C mineralization rates (cf. Sollins et al. 1996; Guggenberger and Kaiser 2003). Iron and Al oxides in particular have the potential to strongly affect DOM abundance and composition through dynamic uptake and release reactions in bioactive systems due to their high specific surface area and abundance of reactive hydroxyl groups.

A considerable amount of prior work has focused on abiotic sorption–desorption in model (oxy)hydroxide systems where strong bond formation and DOM molecular fractionation have been observed. For example, goethite (α-FeOOH) surface Fe atoms form inner-sphere complexes with DOM carboxyl groups via ligand-exchange with surface hydroxyls, and the associated sorption reactions are often irreversible or hysteretic (Gu et al. 1994; Chorover and Amistadi 2001; Fu and Quan 2006, Kaiser et al. 2007). Goethite surfaces have been shown to preferentially sorb DOM molecules of high molar mass (Chorover and Amistadi 2001; Ohno et al. 2007) that are relatively enriched in N and P (Ognalaga et al. 1994; Celi et al. 1999; Omoike and Chorover 2006). Gibbsite (γ-$Al(OH)_3$) also forms strong surface bonds with organic matter (Guan et al. 2006), and its sorption affinity for P compounds is comparable to that of goethite (Shang et al. 1996; Stevenson and Cole 1999). In addition, gibbsite has the potential to influence microbial community structure and function as a source of bioaccessible Al, which can decrease microbial growth and respiration through toxicity effects (Wood 1995; Fischer et al. 2002; Schwesig et al. 2003). By comparison, primary tectosilicate surfaces such as that of quartz (α-SiO_2), are much less reactive toward DOM because of their lower hydroxyl site density (much of the surface is dominated by siloxane sites),

their greater surface acidity (lower point of zero charge), and lower specific surface area.

Prior abiotic sorption studies have provided an improved understanding of the chemical mechanisms of interaction between organics and (oxy)hydroxide surfaces. However, the interaction of these sorption reactions with nutrient cycling processes in bioactive mineral-microbe systems has not been addressed, especially in regards to the influence on (and effects of) microbial community composition, and how these interactions may change over time and with increasing degree of organic matter decomposition. To address this, we used a controlled laboratory incubation with native forest soil microbial inoculum to evaluate the influence of goethite and gibbsite surfaces on soluble or "water extractable" organic matter (WEOM) quality, organic C mineralization rates, and changes in microbial community composition. The incubation was carried out over 154 days to assess time dependent controls of oxide surfaces on soluble nutrients and microbial communities. By examining both dissolved organic C compounds and decomposer community composition, we had the unique opportunity to track the relationships between changes in microbial communities and substrate chemistry over time. The current study builds on a recently published analysis of the physiochemical characteristics of the WEOM deriving from the same set of incubation experiments; those data (Heckman et al. 2011) are used here to help explain variation in microbial community composition and nutrient dynamics over time.

Methods

Experimental design

Natural forest floor organic material was incubated in the presence of three matrix types to assess the influence of goethite and gibbsite relative to pure quartz (α-SiO_2) on WEOM characteristics throughout the degradation process. The matrices for each treatment were as follows: (i) Control treatment: 30 g quartz sand; (ii) Goethite treatment: 6 g goethite grains and 24 g quartz sand; and (iii) Gibbsite treatment: 6 g gibbsite grains and 24 g quartz sand. Goethite and gibbsite were purchased from Ward's Natural Science (Rochester, NY). Quartz sands were purchased from Fisher Scientific (Pitsburgh, PA). All minerals were devoid of detectable impurities as determined by X-ray diffraction. Particle size and specific surface area varied among the minerals. Quartz, goethite, and gibbsite particles had mean diameters of 211, 23, and 14 μm and specific surface areas of 0.03, 3.51, and 1.32 $m^2\ g^{-1}$, respectively (Heckman et al. 2011).

Organic material used in the incubation experiment consisted of partially decomposed forest floor material (composite of O_i, O_e, O_a horizons) collected from an Arizona *Pinus ponderosa* forest. Forest floor material was dried at 30°C, cut to pieces measuring $\sim$1 cm, and homogenized using a blender. Three grams of homogenized forest floor material were mixed with the respective quartz sand, gibbsite or goethite treatments in 125 ml glass jars (Fisherbrand, Fisher Scientific). Microbial inoculum from the O horizon material was extracted following Wagai and Sollins (2002). Freshly collected forest floor material was mixed with deionized water at a weight to volume ratio of 1:5. The mixture was shaken vigorously for 30 min on a reciprocal shaker followed by overnight shaking on a low frequency setting. After 12 h of slow shaking, the mixture was vacuum filtered through a 5 μm polycarbonate membrane filter. Vacuum line pressure was kept below 69 kPa to prevent lysing of microbial cells. The filtrate was stored in a sterilized bottle overnight at 4°C before use. A 1 ml aliquot of inoculum solution was added to each jar. Samples were then homogenized, wetted to 60% of water holding capacity (Cassel and Nielsen 1986) with deionized water, and tamped to a uniform bulk density. Sample cups were placed in 950 cm^3 mason jars. Soil moisture was maintained by the addition of 3 ml of water to the bottom of each jar to maintain 100% relative humidity within the jar atmosphere. Aerobic conditions in the sample jars were maintained by venting the samples periodically.

Mason jars were fitted with septa to allow for headspace sampling. Headspace samples were collected every 2–3 days by removal of a 1 ml aliquot of headspace gas using a syringe. Headspace CO_2 concentration was measured using an Infra-Red Gas Analyzer (Qubit CO_2 Analyzer, Kingston, ON, Canada). Jars were ventilated after each headspace measurement.

Samples were incubated at 25°C for seven time intervals: 5, 10, 20, 30, 60, 90 and 154 days. Each time

interval was replicated three times for a total of 63 samples. All 63 samples were prepared at the same time. At the end of each time interval, three replicates from each treatment were destructively sampled. Samples were mixed with a spatula until homogenized, then 12 g subsamples of material were removed and frozen at −10°C for microbial analysis at a later time. The remainder of the sample was mixed with deionized water in a 15:1 solution to solid ratio and shaken on a side-to-side shaker for 24 h. Samples were vacuum filtered, first over a 1 μm glass fiber A/E filter, then over a 0.22 μm polymer filter (Millipore type GV). The filtrate containing soluble inorganic ions in addition to the WEOM fraction was stored in sterilized bottles at 4°C until analyses were completed. In this experiment, the WEOM fraction is used as a proxy for the DOM fraction found in natural environments.

WEOM analysis

Total organic (non-purgeable) carbon and total nitrogen of the WEOM solutions were measured on a Shimadzu TOC-VCSH analyzer (Columbia, MD). Inorganic anions (NO_3^-, NO_2^-, PO_4^{3-}) were measured by ion chromatography (Dionex Ion Chromatograph DX-500, Sunnyvale, CA) using the Ion Pac AS11 column with a guard column (AG11) and sodium hydroxide (50 mM) as the mobile phase. Select samples were analyzed for ammonium using the Berthelot reaction (Forster 1995). Concentrations of ammonium were below detection limits (<0.02 ppm), and therefore ammonium measurements were not carried out on the full sample set. Organic nitrogen was calculated by subtracting NO_3^- and NO_2^- from total nitrogen. Total phosphorus was measured by Inductively Coupled Plasma Mass Spectrometry (ICP-MS) using a Perkin Elmer Elan DRC II ICP-MS (Waltham, MA). Organic P was calculated as the difference between total phosphorus and orthophosphate. C:N:P ratios were calculated using total C, total N and total P.

In a prior report (Heckman et al. 2011), WEOM solutions were characterized by DRIFT (diffuse reflectance infrared fourier transform spectroscopy) and TG/DTA (thermogravimetry/differential thermal analysis). Additionally, measurements of apparent molar mass, pH, electrical conductivity, dissolved Fe and dissolved Al were conducted on WEOM solutions. A concise summary of the most relevant data is included in Table 3.

Microbial community analysis

Shifts in bacterial and fungal community structure were evaluated over the course of the incubation (days 5, 20, 60, 90, and 154) using bacterial tag-encoded FLX amplicon pyrosequencing (bTEFAP), a universal bacterial identification method, and fungal tag-encoded FLX amplicon pyrosequencing (fTEFAP), a universal fungal identification method. The fTEFAP and bTEFAP methods were conducted by the Research and Testing Laboratory, Lubbock, Texas as described elsewhere (Acosta-Martinez et al. 2008). Briefly, DNA was extracted from approximately 0.5 g of soil using the Fast DNA Spin Kit for soil (QBIOgene, Carlsbad, CA) following the manufacturer's instructions. The 16S universal Eubacterial primers 28F (GAGTTTGATCNTGGCTCAG) and 519R (GTNTTACNGCGGCKGCTG) were used for amplifying the ~500 bp region of bacterial 16S rRNA genes. For analysis of the fungal 18S rRNA gene, the primers funSSUF (5′-TGGAGGGCAAGTCTGGTG-3′) and funSSUR (5′-TCGGCATAGTTTATGGT-TAAG-3′) were used (Rousk et al. 2010). All primers contained a 12 basepair barcode to identify the original sample. HotStarTaq Plus Master Mix Kit (Qiagen, Valencia, CA) was used for PCR under the following conditions: 94°C for 3 min followed by 32 cycles of 94°C for 30 s; 60° C for 40 s and 72°C for 1 min; and a final elongation step at 72 C° for 5 min. Equal volumes of the amplicon products were then pooled, and purified using Agencourt Ampure beads (Agencourt Bioscience Corporation, MA, USA). DNA amplicons were then sequenced using a 454 Genome Sequencer FLX System (Roche, Nutley, New Jersey).

Statistical methods

Calculation of CO_2 respired throughout the incubation followed Zibilske (1994). Percent CO_2 was converted to mass of C and normalized to the C content of the sample prior to incubation (mg C g^{-1} sample C). Nonlinear regression was used to fit a first order decay model to C mineralization data (Rasmussen et al. 2006). The model that gave the best fit consisted of two pools that both exhibited first order decay, a faster-cycling "labile" pool and a slower-cycling "recalcitrant" pool: $-dC/dt = C_L e^{-k_L t} + C_R e^{-k_R t}$, where *-dC/dt* is [mg C g^{-1} sample C h^{-1}], C_L and C_R are the decomposition rates of the labile and

recalcitrant pools of C, and k_L and k_R are the decomposition rate constants (hr^{-1}) for the C pools. The total pool size (mg C g^{-1} sample C) for each soil C pool, C_{LT} and C_{RT}, respectively, was estimated by integrating the area under the curve for each pool: $C_{TL} = C_L/k_L\left(1 - e^{-k_L t}\right)$, and $C_{TR} = C_R/k_R\left(1 - e^{-k_R t}\right)$. The statistical software program, JMP, was used for estimation of model parameters and their associated error terms.

Each sample harvested at a specific destructive sampling period was treated as a replicate for a given treatment, providing three replicates for each treatment per sample time and a total of 21 replicates per treatment across all time periods. Significant differences between WEOM solution properties among treatments were determined by two-way ANOVA using mineral treatment (goethite, gibbsite or control) and time as the main effects followed by Tukey–Kramer post hoc test at a 95% confidence limit ($n = 21$ for each mineral treatment). A time × treatment interaction term was included in ANOVA analyses, but was never statistically significant.

Differences within and between microbial communities were determined by analysis of the relative abundance of species frequencies and analyzed relative to time, mineral composition, and solution chemistry in the multivariate statistical software package PC-ORD version 5 software (McCune and Mefford 2006). Pairwise community distances were estimated with the Sørensen (Bray-Curtis) index and ordinated with nonmetric multidimensional scaling (NMS). NMS is an iterative, best-fit technique that arranges samples in space so that the distance between each pair of samples is in rank order with their similarities in species composition. The optimal number of dimensions (k) was selected based on a Monte Carlo test of significance at each level of dimensionality comparing 250 runs with empirical data against 250 randomized runs with a step-down in dimensionality from 6 to 1 and a random seed starting value. For the bacterial communities, the k = 1 and k = 2 dimensional solutions produced the best solutions with stress values smaller than those in randomized runs ($P = 0.004$). For ease of interpretation, the two-dimensional solution was selected and the data re-ordinated with k = 2 configuration using the seed generated from the K 2 dimensional solution, a stability criterion at 0.0000001, 100 iterations to evaluate stability. For the fungal communities, the k = −2 dimensions produced the best solutions with a stress value smaller than those in randomized runs ($P = -0.004$). The data was then re-ordinated following the same steps.

Relationships between communities and WEOM solution properties measured during the incubation were assessed by overlays or joint biplots of those variables, which included mineral treatment, length of incubation (Time), pH, EC, total organic C, total N, apparent molecular weight (Mw), NO_2^-, NO_3^-, PO_4^{3-}, Al, Fe, and total P. The angle and length of the lines on the biplots indicate the direction and strength of the correlation among variables and microbial community. Varimax rotation on the ordination axes was used to maximize variance explained by the most significant correlation vectors. Univariate relationships between the newly rotated ordination scores and environmental variables were examined with Pearson's correlation coefficient in JMP 7.0 (SAS Institute, Cary NC).

A multiresponse permutation procedure (MRPP) using Sørensen's distance and rank transformation was used to examine statistical significance between communities from different treatments and incubation lengths. MRPP produces a test statistic *A* which ranges from −1 and 1. Objects that are more dissimilar between groups than within groups are indicated by an *A* statistic greater than 0.

Results

Phosphorus dynamics

Average values of both total P and orthophosphate were significantly lower in the oxide treatments than in the control (control^A > goethite^B = gibbsite^B, Fig. 1). Amounts of orthophosphate were below detection level (0.34 μM) in the oxide treatments for all sampling periods except day 30 in the goethite treatment when very low levels of orthophosphate were measured in one of the replicates. Total P concentrations in the control treatment were higher than in the oxide treatments, approximately ~1.25–2.75 μmol g^{-1} C, and the control also showed an increase in P content on Day 154 of approximately 3.0 μmol g^{-1} C (Table 1). Similarly, organic P concentrations in the oxide treatments were low throughout the incubation, with values around

0.2–0.4 μmol g^{-1} C, until Day 154 when a dramatic increase of ~1.2 μmol P g^{-1} C was observed.

Carbon dynamics: DOC concentrations and respiration rates

DOC concentrations were lower in the oxide treatments than in the control when averaged over time (Table 1). This difference was mainly the result of two large, but reproducible, spikes in C concentration at days 20 and 60 in the control treatment (Fig. 2). By day 154, there was no significant difference in DOC concentrations among the control and oxide treatments. DOC concentrations decreased by approximately 50% over the course of the incubation in both the control and oxide treatments, though DOC concentrations of the control treatment exhibited larger fluctuations over time than the oxide treatments.

Respiration rates were similar among treatments (Fig. 3; Table 2). Approximately 15% of the total substrate C was respired over the 154 day period in all treatments. The total amount of C respired by the gibbsite treatment was statistically lower than the amount of C respired by the control treatment (153 ± 6 and 173 ± 5 mg C, respectively). Respiration rate model parameters indicated that the labile pool of C (C_{LT}) was larger in the gibbsite treatment than in the control and goethite treatment, while the recalcitrant pool (C_{RT}) was smaller (Table 2). However, differences in respiration rate parameters were not significant.

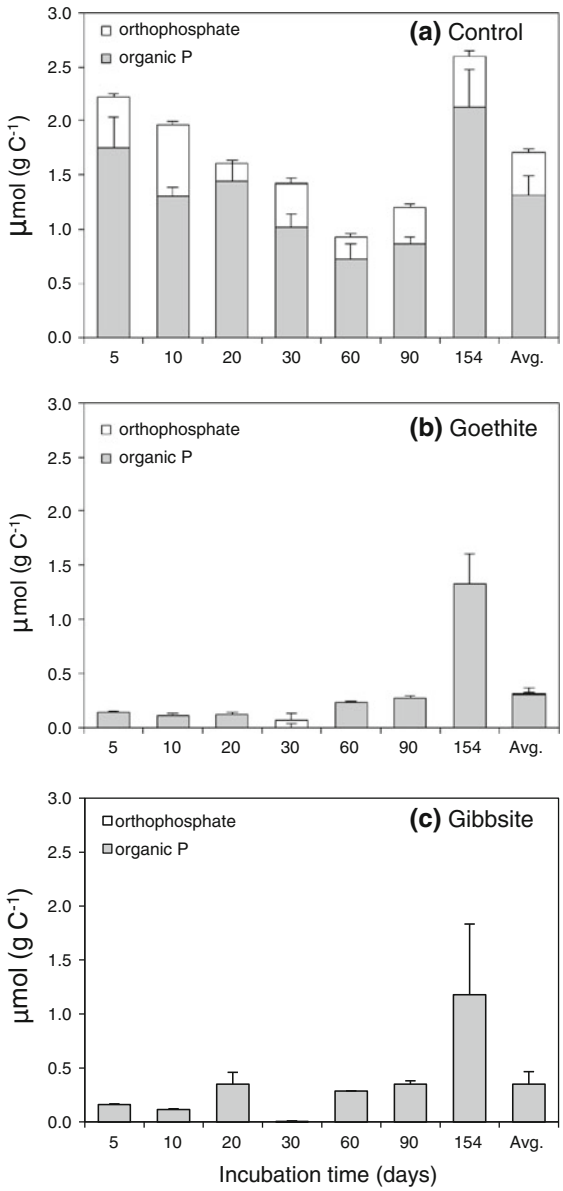

Fig. 1 Changes in orthophosphate and organic P content of WEOM solutions over time. The P contents of the solutions were normalized to the respective C content of the solid sample prior to incubation

Nitrogen dynamics

Total soluble N concentrations were not significantly different among the treatments when averaged over time, ranging from 17 ± 5, 13 ± 6, and 13 ± 4 μmol N g^{-1} C for control, goethite, and gibbsite, respectively. However, relative concentrations of nitrate, nitrite, and total N fluctuation patterns did show differences among the treatments (Fig. 4), and concentrations of nitrate were significantly higher in the goethite treatment than in the control with values of 2.82 ± 0.47 and 1.25 ± 0.24 μmol N g^{-1} litter C, respectively.

C:N:P ratios of WEOM solutions

The carbon to phosphorus (C:P) molar ratio serves as an apparent predictor of P mineralization and/or immobilization during forest floor decomposition (Blair 1988). Saggar et al. (1998) suggested a critical forest floor C:P molar ratio of 550 for net P mineralization. In the oxide treatments, C:P molar ratios of WEOM were well above this critical value throughout the incubation until day 154 when they declined sharply by an order of magnitude (Table 1). In

Table 1 Characteristics of water extractable organic matter (WEOM) solutions over time

Treatment	Incubation length Days	Organic C ^mmol $g_{litter\ C}^{-1}$	Total N	NO_3^-	NO_2^- ^μmol $g_{litter\ C}^{-1}$	Total P	PO_4^{3-}	C:N Molar ratios	C:N:P
Control	5	1.48 (0.29)	10.63 (0.82)	0.00	0.33 (0.18)	2.22 (0.31)	0.48 (0.03)	139 (24)	666:5:1
	10	1.08 (0.14)	13.96 (2.39)	1.99 (0.44)	0.18 (0.06)	1.97 (0.10)	0.66 (0.03	77 (14)	546:7:1
	20	3.42 (1.01)	13.22 (2.10)	0.05	0.37 (0.13)	1.61 (0.14)	0.17 (0.03)	259 (80)	2,123:8:1
	30	0.67 (0.21)	13.55 (2.45)	2.31 (0.72)	0.15 (0.01)	1.42 (0.17)	0.4 (0.05)	50 (18)	472:10:1
	60	3.89 (0.50)	37.83 (1.57)	1.26 (0.17)	0.05	0.93 (0.16)	0.21 (0.03)	103 (8)	4,172:41:1
	90	0.84 (0.07)	11.76 (1.12)	1.02 (0.22)	0.59 (0.10)	1.21 (0.09)	0.34 (0.03)	72 (12)	696:10:1
	154	0.48 (0.01)	15.19 (0.66)	2.11 (0.15)	0.46 (0.14)	2.60 (0.39)	0.47 (0.05)	32 (13)	186:6:1
	Average over time	**1.69 (0.32)^{A}**	**16.59 (5.39)^{A}**	**1.25 (0.24)^{B}**	**0.30 (0.09)^{A}**	**1.71 (0.14)^{A}**	**0.39 (0.03)^{A}**	**102 (21)^{A}**	**1,266:12:1**
Goethite	5	1.26 (0.22)	8.43 (0.96)	0.46 (0.46)	0.34 (0.18)	0.14 (0.02)	0.00	150 (30)	8,969:60:1
	10	0.80 (0.13)	11.36 (1.16)	2.13 (0.62)	0.27 (0.07)	0.12 (0.02)	0.00	70 (13)	6,839:97:1
	20	1.20 (0.12)	32.15 (6.53)	7.16 (0.62)	0.29 (0.19)	0.12 (0.02)	0.00	37 (9)	9,742:261:1
	30	0.94 (0.27)	6.69 (0.21)	2.29 (0.45)	0.11 (0.04)	0.03 (0.02)	0.07 (0.07)	94 (25)	34,619:369:1
	60	0.60 (0.19)	3.20 (0.50)	3.14 (0.50)	0.06 (0.01)	0.24 (0.01)	0.00	188	2,523:13:1
	90	0.69 (0.12)	10.32 (0.01)	1.45 (0.28)	0.45 (0.08)	0.28 (0.02)	0.00	67 (1)	2,480:37:1
	154	0.34 (0.03)	15.23 (1.27)	3.13 (0.35)	0.31 (0.11)	1.33 (0.27)	0.00	22 (2)	254:11:1
	Average over time	**0.83 (0.09)^{B}**	**12.36 (5.70)^{A}**	**2.82 (0.47)^{A}**	**0.26 (0.10)^{A}**	**0.32 (0.10)^{B}**	**0.01 (0.01)^{B}**	**64 (16)^{A}**	**9,347:121:1**
Gibbsite	5	0.96 (0.14)	12.57 (2.98)	0.04 (0.04)A	0.56 (0.17)	0.16 (0.01)	0.00	76 (22)	5,924:78:1
	10	0.88 (0.15)	9.39 (0.79)	1.11 (0.52)	0.38 (0.10)	0.12 (0.01)	0.00	93 (21)	7,554:81:1
	20	1.40 (0.60)	22.07 (8.89)	3.20 (3.20)	0.00	0.35 (0.11)	0.00	64 (52)	4,004:63:1
	30	0.58 (0.09)	10.53 (0.68)	2.13 (0.15)	0.08 (0.02)	0.01	0.00	55 (4)	85,406:1539:1
	60	0.98 (0.15)	9.97 (4.97)	3.21 (0.49)	0.08 (0.02)	0.29	0.00	84 (1)	3,405:35:1
	90	0.46 (0.04)	9.34	1.59 (0.20)	1.41 (1.01)	0.35 (0.03)	0.00	49 (4)	1,304:27:1
	154	0.35 (0.01)	18.61 (0.89)	4.16 (0.28)	0.25 (0.05)	1.18 (0.65)	0.00	19 (12)	267:16:1
	Average over time	**0.80 (0.11)^{B}**	**13.21 (4.38)^{A}**	**2.21 (0.70)^{AB}**	**0.40 (0.20)^{A}**	**0.35 (0.11)^{B}**	**0.00^{B}**	**61 (10)^{A}**	**15,414:263:1**

^Specifically: measured as milli/micromoles of the nutrient of interest in the dissolved organic matter fraction, normalized to the total grams of C in the solid sample prior to incubation. Values at each time point are the average of three replicates for each treatment ($n = 3$). "Average over time" values are the average of all replicates across time ($n = 21$). Values in parenthesis are the standard error of replicates ($n = 3$ or $n = 21$), where parenthesis are not shown the standard error was zero. Significance was determined using two-way ANOVA with treatment and time as main effects, followed by Tukey's HSD post hoc test ($\alpha = 0.05$). Within each column, means followed by different superscript letters are significantly different

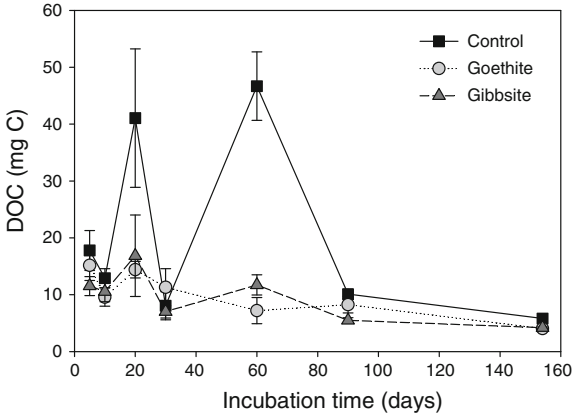

Fig. 2 Changes in dissolved organic C (DOC) content of the WEOM solutions over time. The DOC contents of the solutions were normalized to the grams of C in each solid sample prior to incubation. *Bars* represent the standard error of 3 replicates

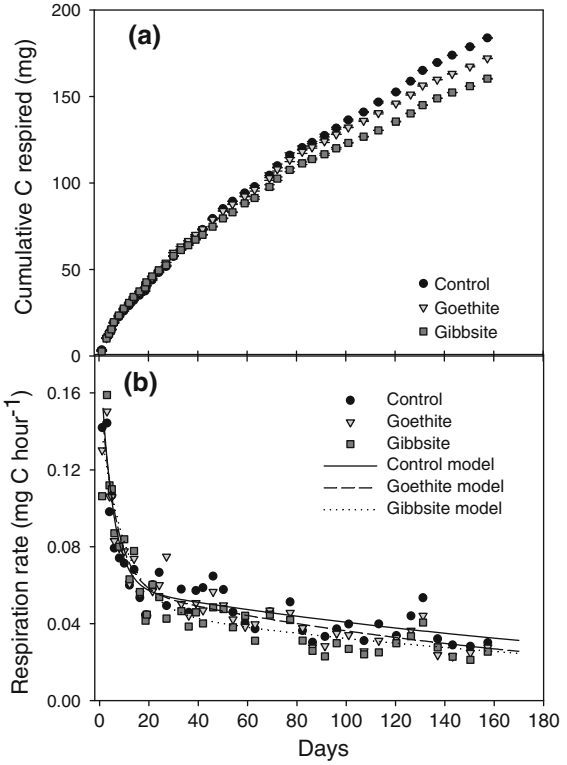

Fig. 3 All respiration parameters and measurements are normalized to the grams of C in each sample prior to incubation. **a** Cumulative mg C respired over the length of the incubation. *Bars* are the standard error of all available replicates (number of replicates decreased over time due to destructive sampling). **b** Change in respiration rates over the length of the incubation. Symbols are the average respiration rate for each treatment and sampling time. *Lines* are the two-pool models fit to the measured data

general, C:P molar ratios of WEOM solutions from the control treatment were lower than in the oxide treatments and often dipped below the critical C:P molar ratio of 550.

The generally accepted critical C:N value for N limitation is approximately 30. At C:N ratios above 30 net immobilization dominates, while at C:N ratios below 20 mineralization dominates (Stevenson and Cole, 1999). C:N ratios were above the critical 30:1 value until day 154 of the incubation across all treatments.

Microbial community composition

Analysis of the pyrosequencing data indicated that length of incubation was a dominant factor in structuring both bacterial and fungal communities (Figs. 5, 6). NMS ordinations fit both bacterial and fungal datasets well (stress = 4.3, $P = 0.004$, stress = 7.6, $P = 0.004$, respectively). Note that P values given in reference to NMS ordination fits do not denote significant differences among treatment groups, but are rather related to the fit of the overall data set to the defined axes. However, the *P* values given in reference to correlations among WEOM properties and NMS axes do denote significance of correlation.

For bacterial communities (Fig. 5), the primary axis correlated strongly with length of incubation ($r = 0.89$, $P < 0.0001$), but showed moderate and significant correlation to other WEOM solution qualities including pH ($r = 0.48$, $P = 0.0009$), EC ($r = -0.43$, $P = 0.0036$), and Mw_{APP} ($r = 0.57$, $P < 0.0001$). Axis 2 exhibited strong-to-moderate significant positive correlations with concentrations of total P ($r = 0.60$, $P < 0.0001$), PO_4 ($r = 0.79$, $P < 0.0001$), and organic C ($r = 0.36$, $P = 0.015$). According to the MRPP, bacterial communities differed significantly by incubation time ($A = 0.49$, $P < 0.01$). All pairwise comparisons of the communities from different lengths of incubation (sampling dates) were significantly different except for days 60 and 90. Significant differences among communities according to sampling date are indicated by dashed circles in Fig. 5. Because of the overwhelming dominance of time as a factor influencing variance in microbial community, MRPP did not indicate a statistical difference among communities by mineral treatment. However, communities clearly appeared to

Table 2 Respiration rate data

Treatment	Total C Respired* mg C	Avg Resp. Rate* mg C hr^{-1}	C_L $g_{C(resp)}$ $g_{C(litter)}^{-1} hr^{-1}$	k_L hr^{-1}	C_R $g_{C(resp)}$ $g_{C(litter)}^{-1} hr^{-1}$	k_R h^{-1}	Pool sizes (mg C)	
							C_{LT}	C_{RT}
Control	173 (±5)^{A}	0.0117 (±0.0003)^{A}	0.285 (0.114)^{A}	0.0185 (0.0047)^{A}	0.0656 (0.0038)^{A}	0.00021 (0.00004)^{A}	15.4 (7.3)^{A}	167.8 (62.2)^{A}
Goethite	163 (±8)^{AB}	0.0111 (±0.0002)^{AB}	0.247 (0.073)^{A}	0.0157 (0.0034)^{A}	0.0651 (0.0038)^{A}	0.00026 (0.00004)^{A}	15.8 (5.8)^{A}	153.2 (41.2)^{A}
Gibbsite	153 (±6)^{B}	0.0107 (±0.0002)^{B}	0.227 (0.057)^{A}	0.0133 (0.0029)^{A}	0.0639 (0.0045)^{A}	0.00030 (0.00005)^{A}	17.1 (5.7)^{A}	142.3 (38.5)^{A}

*Values calculated as the mean of the 3 experimental replicates per treatment that were incubated for the full 154 day period

Values given are normalized to the grams of C present in each sample prior to incubation. Respiration rate parameters are fit according to the following function: $y = C_L e^{-kLt} + C_R e^{-kRt}$. Significance was determined using one-way ANOVA by treatment, followed by Tukey's HSD post hoc test ($\alpha = 0.05$). Within each column, means followed by different superscript letters are significantly different. Values in parentheses are the standard error of the measurements and parameters

cluster visually by mineral treatment, and further statistical analysis indicated that when examined by sampling date, communities from different mineral treatments were statistically different from one another.

For fungal communities (Fig. 6), the primary axis also correlated primarily with incubation length ($r = 0.84$, $P < 0.0001$), and moderately to weakly with Mw_{APP} ($r = 0.51$, $P = 0.0003$), pH ($r = 0.46$, $P = 0.0016$) and EC ($r = -0.35$, $P = 0.017$). Axis 2 exhibited a moderate negative correlation with organic C concentrations ($r = -0.48$, $P = 0.0008$). According to the MRPP, fungal communities also differed significantly by incubation time ($A = 0.37$, $P > 0.01$) and all pairwise comparisons among different incubation times were significantly different except for days 60, 90, and 154. Significant differences among communities according to sampling date are indicated by dashed circles in Fig. 6. Although MRPP did not indicate significant separation by mineral treatment, communities from the goethite and gibbsite treatments appeared to cluster separately from the control. Similar to the statistics for the bacterial communities, fungal communities from the oxide treatments were statistically different from control communities when examined by individual sampling date.

Discussion

Influence of oxide surfaces on soluble nutrient dynamics

Phosphorus

The presence of geothite and gibbsite had the strongest effects on total P and orthophosphate concentrations but also influenced N and C concentrations to a lesser degree (Table 1). Assuming equivalent soluble releases from forest floor organic matter, essentially all orthophosphate and 75% of organic P were removed from solution in the oxide treatments, most likely through sorption to oxide and organic matter surfaces and possibly through formation and precipitation of metal-P complexes (Gerke 2010). It is well established that P may be removed from active cycling through sorption to oxide surfaces (Stevenson 1994; Stevenson and Cole 1999). Both inorganic P (HPO_4^{2-}, $H_2PO_4^{-}$) and organic P (biomolecules) may form strong bonds with

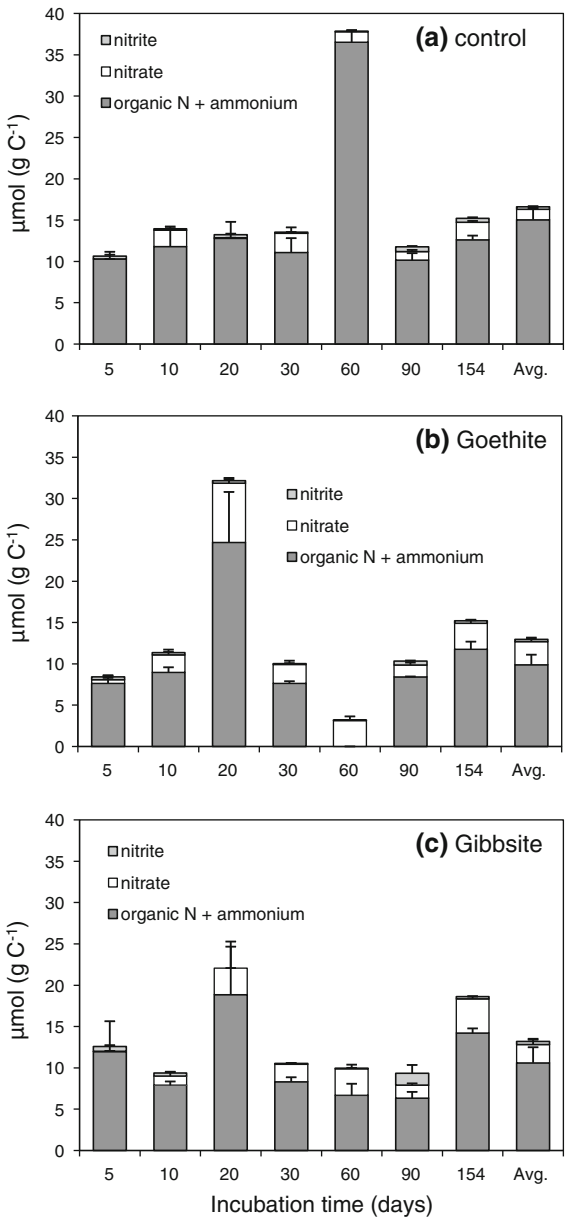

Fig. 4 Changes in nitrate, nitrite and organic N^+ ammonium content of WEOM solutions over time. The N contents of the solutions were normalized to the respective C content of the solid sample prior to incubation

oxide surfaces through ligand exchange and metal bridging (Gerke and Hermann 1992), and the strength of phosphate fixation is approximately equal for goethite and gibbsite (Stevenson and Cole 1999). Changes in microbial community composition along with increases in organic matter decomposition could also have influenced P concentrations in WEOM solution (Hunt et al. 2007). However, given the well-documented affinity of oxide surfaces for P, it seems more likely that sorption was the dominant processing influencing P concentrations in WEOM solutions.

The data suggest phosphorus limitation had a significant effect on microbial community composition throughout the incubation. Correlation analyses suggest bacterial communities were more sensitive to P limitation than fungal communities, as evidenced by strong correlation between total P concentration and variation in bacterial community composition that was absent with fungal community variation (Figs. 5, 6). Furthermore, total P and orthophosphate concentrations were the dominant WEOM solution chemical properties separating bacterial communities among treatments, and they significantly affected bacterial community composition regardless of incubation time. In general, fungi have lower nutrient requirements than bacteria (Smith 2002), and the greater ability of fungal communities to cope with P limitation may explain the lack of correlation between P concentrations and variation in fungal community composition.

Carbon

When averaged over time, total organic C concentrations in WEOM solutions from the oxide treatments were half that observed for the control (Table 1). Though differences in dissolved organic C concentration among the treatments may be partially attributed to differences in microbial degradation rates and incorporation of C into microbial biomass, it is likely that variation in sorptive affinity of dissolved C for the (oxy)hydroxide surfaces played a dominant role. Surface hydroxyl groups of gibbsite and goethite surfaces are known to form bonds with organic molecules through ligand exchange reactions with organic phosphoryl (Omoike and Chorover 2006), carboxylate and (to a lesser extent at circumneutral pH) phenolate groups (Parfitt et al. 1977; Gu et al. 1994; Molis et al. 2000; Amistadi and Chorover 2001; Schneider et al. 2010). Once such stable inner-sphere complexes are formed, they are slow to dissociate even with a reduction in aqueous phase DOC concentrations, and have been shown to persist and strengthen over time (Gu et al. 1994; Kaiser et al. 2007; Journey et al. 2010). If it is assumed that once formed, DOC-oxide complexes are stable over the period of incubation, then the

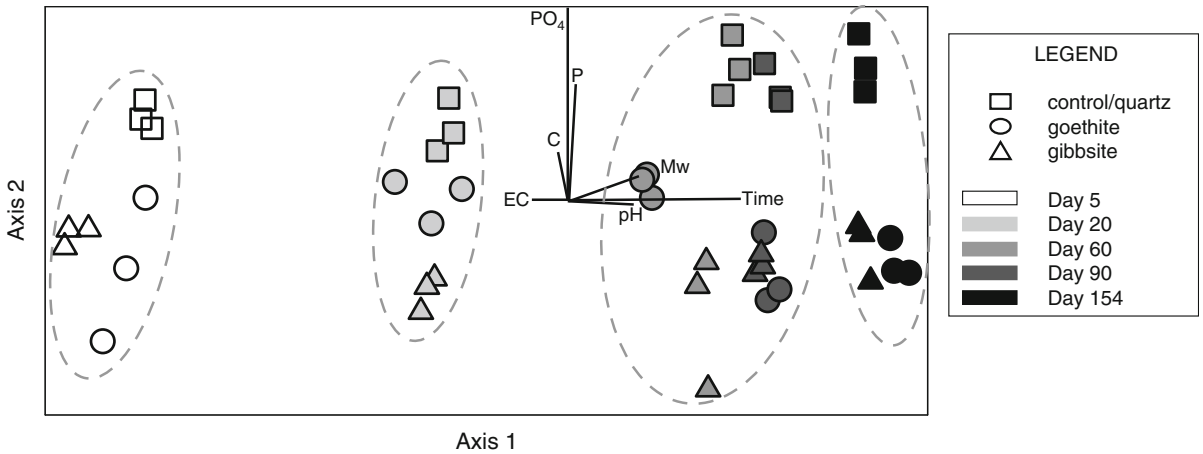

Fig. 5 Non-metric multidimensional scaling ordination of *bacterial* pyrosequencing data. Symbols code for treatment (control *square*, goethite *circle*, gibbsite *triangle*). *Colors code* for length of incubation. *Lines* show correlation vectors of the measured WEOM properties with the ordination: EC, C (organic C), PO_4, P (total P), Mw, pH, Time (length of incubation). The final solution has two dimensions (stress = 4.3, $P = 0.004$). *Circles of dashed lines* are drawn around data points to indicate statistical differences among communities grouped by sampling date

reproducible fluctuations in DOC (Fig. 2) are the result of microbial processes. Differences in dissolved organic C concentrations among treatments were most pronounced on days 20 and 60 of the incubation (Fig. 2). We hypothesize that these large 'flushes' of C in the control treatment were representative of microbial biomass turnover events when large changes in community size or composition took place. Furthermore, we postulate that similar biomass turnover events were taking place in the oxide treatments, but that the solubilized C was rapidly sorbed by the oxide surfaces (McKnight et al. 1992; Day et al. 1994) and therefore not detected in the WEOM extractions. The NMS plots of variation in fungal community composition (Fig. 6) shows that variation in fungal communities along axis 2 was primarily correlated with concentration of dissolved organic C. This may support the above hypothesis, and indicate that changes in DOC concentrations were the result of microbial cell lysis and turnover. Alternatively, the correlation between DOC concentration and fungal community composition could indicate that community composition was changing as a result of changes in dissolved organic C availability. Given that forest floor material was present in the microcosms at a 10% by weight proportion and that concentrations of C were much larger than concentrations of N or P, it seems unlikely that C availability was a driver of variation in fungal community composition. The same may be true for bacterial communities. Variation in bacterial community composition was also correlated, though weakly, with DOC concentration along axis 2 (Fig. 5).

Microbial community *composition* was significantly affected by the presence of goethite and gibbsite perhaps due to their effects on N and P availability, but *respiration rates* were not, which is suggestive of something akin to functional redundancy. The hypothesis of functional redundancy or functional equivalence is based on the idea that more than one species is capable performing a given function or role within a particular ecosystem or environment (Walker 1992). Indeed, many studies of C mineralization rates in soils have found that even given significant changes in environmental parameters, microbial communities are able to adapt and change such that microbial community structure is significantly different while decomposition and C mineralization rates are unchanged (Griffiths et al. 2000; Griffiths et al. 2001; Ayres et al. 2006; Wertz et al. 2006; Balser and Firestone 2005). These studies suggest something a step beyond functional redundancy or functional equivalence. Specifically they suggest that soil microbial communities can adapt to changing environmental conditions through changes in community composition such that communities operating under substantially different stress levels can all achieve similar C mineralization rates. The observed highly similar respiration rates among all treatments in this study may lend support to this hypothesis.

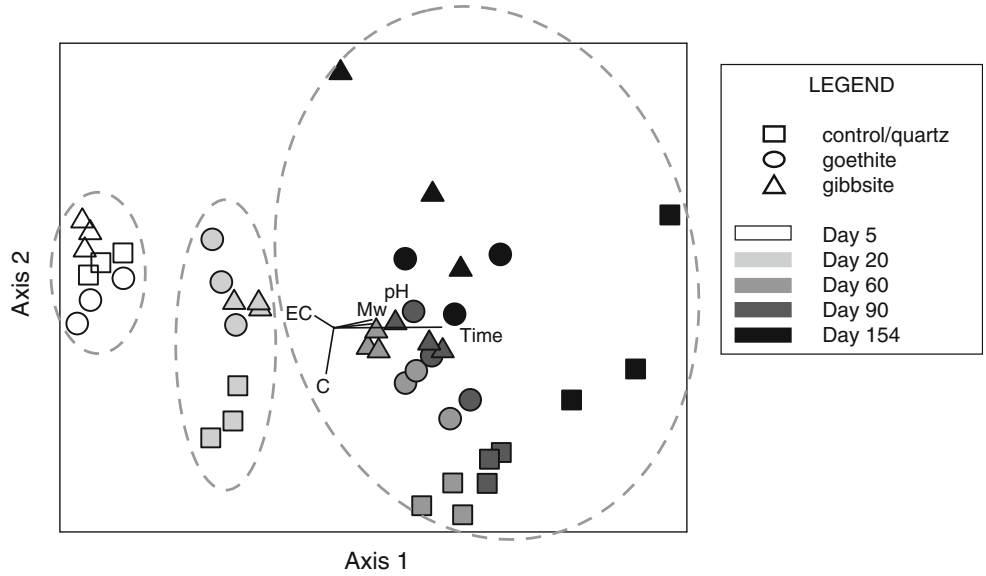

Fig. 6 Non-metric multidimensional scaling ordination of *fungal* pyrosequencing data. Symbols code for treatment (control *square*, goethite *circle*, gibbsite *triangle*). *Colors code* for length of incubation. *Lines* show correlation vectors of the measured WEOM properties with the ordination: EC, Al, C (organic C), Mw, pH, day (length of incubation). The final solution has two dimensions (stress = 7.6, $P = 0.004$). *Circles of dashed lines* are drawn around data points to indicate statistical differences among communities grouped by sampling date

Nitrogen

Aqueous total N concentrations were affected by mineral type to a lesser degree than C and P concentrations. Perhaps the most striking aspect of the nitrogen data time series (Fig. 4) was the large fluctuations in N concentration. The treatments all exhibited one large spike in N content, at day 20 in the oxide treatments and at day 60 in the control. One explanation for the patterns of N concentrations may be microbial turnover and concomitant cell lysis. However, increases in N concentration were not accompanied by similar spikes in either dissolved C or P concentrations. The apparent decoupling of N and C dynamics in dissolved organic matter solutions has been observed previously in many field studies. In experiments in spruce and pine forests, addition of N to soils did not cause observable changes in dissolved organic C yield (Stuanes and Kjønass 1998; Emmett et al. 1998), whereas others note no clear dependence of DOC flux on N availability (Gunderson et al. 1998; McDowell 2002). This apparent decoupling of nutrient dynamics may imply that fluctuations in nutrients are more the product of predator/prey dynamics or shifts in nutrient limitations rather than strictly cell lysis.

Nutrient ratios

Molar ratios of N to P suggested differences in nutrient limitations between the control and oxide treatments, and these differences in nutrient limitations are important due their influence on microbial community composition. Güsewell and Gessner (2009) found that N-limited conditions favor bacteria, while P-limited conditions favor fungi, with the shift from N to P limitation occurring at N:P molar ratios of 15–45. The average total N:P molar ratio of control WEOM was 12, indicating that growth was most likely N-limited throughout the incubation. In contrast, total N:P ratios varied more widely in the oxide treatments, ranging from >1000:1–10:1 (Table 1). Time averaged values were 121 in goethite WEOM and 263 in gibbsite WEOM indicating a prevalence of P-limiting conditions (Table 1).

The critical N:P ratio where nutrient limitation shifts from N to P is not well defined since it depends to a large degree on community composition and the associated species' variance in nutrient requirements, and threshold N:P ratios may be slightly different for WEOM solutions than for solid organics as used in Güsewell and Gessner's (2009) calculations. However, nitrate data may add additional support to the

idea that microbial growth in the oxide treatments was primarily P limited while microbial growth in the control was more N limited. Nitrate and nitrite are typically only formed when N is not limiting, and nitrate concentrations were higher in the oxide treatments than the control throughout the incubation (though only the goethite treatment was statistically significantly higher than the control at the $\alpha = 0.05$ level).

Although there were significant treatment effects on nutrient ratios, general trends were apparent across all treatments. Over time, as decomposition of the forest floor material progressed, molar nutrient ratios (C:N and N:P) declined significantly, and C:N values were an order of magnitude lower at the end of the incubation than at the beginning. The decreases in C:N over time is consistent with an enrichment of microbial-sourced compounds in WEOM solutions. At day 154 of the incubation, C:N values of WEOM solutions were 27, 19, and 16 for control, goethite and gibbsite treatments, respectively. These values are only slightly higher than typical C:N of soil biomass which is usually $\sim$8-12 (Paul and Clark, 1996; Wright and Coleman, 2000). Furthermore, N:P ratios also declined significantly throughout the incubation, and after 154 days were drawing near the global stoichiometric average for forest microbial biomass of 9:1 (Cleveland and Liptzin 2007). In a related study, FTIR analysis of WEOM solutions indicated a steady increase in amide:COO^- and amide:polysaccharide ratios over time in the same samples (Heckman et al. 2011), consistent with accumulation of microbial byproducts produced during cell lysis and turnover. Changes in nutrient ratios together with changes observed in the molecular structure of WEOM over time (see 4.2 below) both indicate an enrichment of microbial biomolecules and metabolites in WEOM solutions with increasing time and degree of biodegradation. This is consistent with research indicating that microbial metabolites comprise a significant portion of dissolved organic matter in natural soil systems (Kalbitz et al. 2000).

Correlations among WEOM solution properties and microbial community composition

Measures of WEOM molecular structure, nutrient content and chemical properties all indicated significant differences in WEOM properties both over time and among mineral treatments. Changes in WEOM properties with increasing time of incubation included a steady increase in aromaticity and Mw_{APP} in all treatments, and a general increase in metal:C ratios in the goethite and gibbsite treatments. Significant differences in WEOM properties among mineral treatments included differences in nutrient limitation as discussed above, and also differences in the structural composition of WEOM solutions. Thermal and FTIR analysis indicated that WEOM from the gibbsite treatment was rich in thermally recalcitrant and carboxyl-rich compounds in comparison to the control treatment, and WEOM from the goethite treatment was significantly depleted in both amide (as a proxy for proteins) and ester (as a proxy for lipids) structures relative to the control WEOM (Table 3) (Heckman et al. 2011).

Significant correlation among community composition variation and WEOM solution properties (Figs. 5, 6) indicated that changes in WEOM were related to changes in microbial community structure. Since microbial communities rely on dissolved organics as a growth substrate, it is likely that changes in microbial communities are indicative of concurrent dynamics in nutrient availability and/or structural lability of dissolved organic molecules (Griffiths et al. 1998; Schutter and Dick 2001). However, it is also likely that differences in community composition among treatments and over time may have led to the production of different biomolecules which would also be reflected as changes in WEOM solution properties (Grandy et al. 2008; Wickings et al. 2011).

Apparent weight averaged molar mass (Mw_{APP}) of WEOM was correlated with variation in community composition along axis 1 in both bacterial and fungal communities. WEOM Mw_{APP} values were positively correlated with dissolved metal to C ratios (Heckman et al., 2011), suggesting that bonding of dissolved organics with dissolved metals contributed to Mw_{APP} values. Correlation between Mw_{APP} and community composition could therefore indicate that the presence of metal-humus complexes accounted for a portion of the influence of Mw_{APP} on community composition, since formation of metal-humus complexes induces chemical and conformational changes that reduce SOC bio-availability (Baldock and Skjemstad 2000; Nierop et al. 2002; Scheel et al. 2007; Mikutta et al. 2011). Alternatively, correlations between community composition and Mw_{APP} could indicate that WEOM

Table 3 Summary data from Heckman et al. 2011

	TG/DTA analysis				Dissolved metals		pH	Mw_{app} Daltons	FTIR peak area differences	
	Enthalpy	% of total mass loss per peak			Fe:C	Al:C			Amide I	Esters
	kJ $g_{mass\ loss}^{-1}$	Exo_1	Exo_2	Exo_3	$mmol_{Fe}:mol_{DOC}$	$mmol_{Al}:mol_{DOC}$			1650 (cm^{-1})	1730 (cm^{-1})
Control	16.6 (2.4)	41 (6)	39 (8)	19 (3)	0.19 (0.06)^{B}	0.97 (0.28)^{B}	5.78 (0.16)^{B}	3495 (392)^{A}	A	A
Goethite	23.2 (1.7)	47 (1)	46 (1)		10.91 (4.01)^{A}	0.51 (0.20)^{B}	5.96 (0.12)^{AB}	2056 (193)^{B}	B	B
Gibbsite	16 (1.0)	43 (1)	25 (0)	32 (1)	0.28 (0.07)^{B}	4.24 (0.92)A	6.05 (0.16)^{A}	2654 (393)^{B}	AB	AB

Values are the averages over time for structural and chemical analyses performed on WEOM solutions. Only statistical differences among treatments are given for DRIFT peak areas because data was used only on an intercomparison basis. Significant differences among dissolved metal to C ratios were determined by one-way ANOVA followed by a Tukey–Kramer HSD test at an $\alpha = 0.05$ level. Statistical analysis was not performed on the TG/DTA data

structural lability declined with increasing decomposition in so far as compounds with higher Mw_{APP} are considered less biodegradable (Tate 1987). These changes in WEOM properties may have led to more favorable conditions for fungi as opposed to bacteria with increasing time of incubation due to the greater ability of fungi to break down more condensed and lignin-rich organics (de Boer et al. 2005; Six et al. 2006; van der Heijden et al. 2008). A feedback may also exist wherein more structurally complex and nutrient limited WEOM solutions select for communities dominated by fungi which in turn produce more thermally recalcitrant and higher Mw biomolecules.

Both bacterial and fungal community composition were most strongly influenced by increasing length of incubation. However, bacterial and fungal communities differed somewhat in their response to increasing incubation length. As decomposition progressed, bacterial communities continued to change, whereas fungal communities, when grouped by sampling date, were not significantly different from one another on days 60, 90, and 154 (see circled groupings in Figs. 4, 5).

Solution pH was significantly correlated with changes in both bacterial and fungal community composition over time, consistent with known control of pH over microbial diversity, activity and biomass in both field and laboratory settings (Anderson and Domsch 1993; Schnittler and Stephenson 2000; Bååth and Anderson 2003; Fierer and Jackson 2006). Electrical conductivity of WEOM solutions (EC) was correlated with changes in community composition over time as well. EC of WEOM solutions was not correlated with dissolved metal concentrations, or dissolved C concentrations, perhaps an indication that microbial composition is controlled by a complex array of aqueous geochemical factors.

The results of this study indicate that in a bioactive incubation, time-dependent changes in WEOM composition are not only the product of selective sorption reactions at mineral surfaces, but also likely result from dynamic changes in microbial community composition that coincide with such reactions. A change in microbial community composition is expected to feedback to affect the types of biomolecules and organic metabolites generated over the course of the incubation. Our data showing that WEOM characteristics correlate with microbial community composition are consistent with this scenario.

Summary

The current work indicates that the presence of goethite and gibbsite has specific and significant consequences for the nutrient content and physiochemical properties of WEOM. Results also indicate that these changes in WEOM properties can co-occur with changes in both bacterial and fungal community composition, without resulting in large impacts on system-level microbial respiration, consistent with the hypothesis of functional redundancy. Though previous studies have examined the effects of oxide surfaces on WEOM or DOM characteristics, this study yields unique insight into the ramifications of these changes in WEOM properties for microbial communities. Furthermore, WEOM and microbial community dynamics were examined over a relatively long time period, and the data suggest that oxide surfaces significantly influence microbial communities throughout the degradation process leading to lasting effects on the composition of the decomposer community.

Acknowledgments This study was funded by grant DEB #0543130 from the National Science Foundation. The authors wish to thank Dr. Stuart Grandy and three anonymous reviewers for their thoughtful edits and suggestions which greatly improved the quality of this study.

References

Acosta-Martinez V, Dowd S, Sun Y, Allen V (2008) Tag-encoded pyrosequencing analysis of bacterial diversity in a single soil type as affected by management and land use. Soil Biol Biochem 40:2762–2770

Amistadi MK, Chorover J (2001) Reaction of forest floor organic matter at goethite, birnessite and smectite surfaces. Geochim Cosmochim Acta 65:95–109

Anderson T-H, Domsch KH (1993) The metabolic quotient for CO_2 (qCO_2) as a specific activity parameter to assess the effects of environmental conditions, such as pH, of the microbial biomass of forest soils. Soil Biol Biochem 25:393–395

Ayres E, Dromph KM, Bardgett RD (2006) Do plant species encourage soil biota that specialize in the rapid decomposition of their litter? Soil Biol Biochem 38:183–186

Bååth E, Anderson TH (2003) Comparison of soil fungal/bacterial ratios in a pH gradient using physiological and PLFA-based techniques. Soil Biol Biochem 35:955–963

Baldock JA, Skjemstad JO (2000) Temperature effects on the diversity of soil heterotrophs and the delta C-13 of soil-respired CO_2. Soil Biol Biochem 32:699–706

Balser TC, Firestone MK (2005) Linking microbial community composition and soil processes in a California annual grassland and mixed-conifer forest. Biogeochemistry 73:395–415

Blair JM (1988) Nitrogen, sulfur and phosphorus dynamics in decomposing deciduous leaf forest floor in the southern Appalachians. Soil Biol Biochem 20:693–701

Cassel DK, Nielsen DR (1986) Field capacity and available water capacity. In: Klute A (ed) Methods of soil analysis, Part 1: physical and mineralogical methods, 2nd edn. SSSA Book Series 5. SSSA Inc., Madison, pp 901–926

Celi L, La Macchia S, Ajmone-Marsan F, Barberis E (1999) Interaction of inositol hexaphosphate on clays: Adsorption and charging phenomena. Soil Sci 164:574–585

Chorover J, Amistadi MK (2001) Reaction of forest floor organic matter at goethite, birnessite and smectite surfaces. Geochim Cosmochim Acta 65:95–109

Cleveland CC, Liptzin D (2007) C:N:P stoichiometry in soil: is there a "Redfield ratio" for the microbial biomass? Biogeochemistry 85:235–252

Day GM, Hart BT, McKelvie ID, Beckett R (1994) Adsorption of natural organic matter onto goethite 89:1–13

de Boer W, Folman LB, Summerbell RC, Boddy L (2005) Living in a fungal world: impact of fungi on soil bacterial niche development. FEMS Microbiol Rev 29:795–811

Emmett BA, Reynolds B, Silgram M, Sparks TH, Woods C (1998) The consequences of chronic nitrogen additions on N cycling and soil water chemistry in a Sitka spruce stand, North Wales. For Ecol Manage 101:165–175

Fierer N, Jackson RB (2006) The diversity and biogeography of soil bacterial communities. PNAS 103:626–631

Fischer J, Quintmeier A, Gansel S, Sabados V, Friedrich CG (2002) Inducible aluminum resistance of *Acidiphilium cryptum* and aluminum tolerance of other acidophilic bacteria. Arch Microbiol 178:554–558

Forster JC (1995) Soil nitrogen. In: Alef K, Nannipieri P (eds) Methods in applied soil microbiology and biochemistry. Academic Press, San Diego, pp 79–87

Fu H, Quan X (2006) Complexes of fulvic acid on the surface of hematite, goethite, and akaganeite: FTIR observation. Chemosphere 63:403–410

Gerke J (2010) Humic (organic matter)-Al(Fe)-phosphate complexes: an underestimated phosphate form in soils and source of plant-available phosphate. Soil Sci 175:417–425

Gerke J, Hermann R (1992) Adsorption of orthophosphate to humic-Fe-complexes and to amorphous Fe-oxide. Z Pflanz Bodenkunde 155:233–236

Grandy AS, Neff JC (2008) Molecular C dynamics downstream: the biochemical decomposition sequence and its impact on on soil organic matter structure and function. Sci Total Environ 404:221–244

Grandy AS, Neff JC, Weintraub MN (2007) Carbon structure and enzyme activities in alpine and forest ecosystems. Soil Biol Biochem 39:2701–2711

Grandy A, Sinsabaugh R, Neff J, Stursova M, Zak D (2008) Nitrogen deposition effects on soil organic matter chemistry are linked to variation in enzymes, ecosystems and size fractions. Biogeochemistry 91:37–49

Griffiths BS, Ritz K, Ebblewhite N, Dobson G (1998) Soil microbial community structure: effects of substrate loading rates. Soil Biol Biochem 31:145–153

Griffiths BS, Ritz K, Bardgett RD, Cook R, Christensen S, Ekelund F, Sorensen SJ, Bååth E, Bloem J, de Ruiter PC,

Dolfing J, Nicolardot B (2000) Ecosystem response of pasture soil communities to fumigation-induced microbial diversity reductions: an examination of the biodiversity-ecosystem function relationship. Oikos 90:279–294

Griffiths BS, Ritz K, Wheatley R, Kuan HL, Boag B, Christensen S, Ekelund F, Sorensen SJ, Muller S, Bloem J (2001) An examination of the biodiversity-ecosystem function relationship in arable soil microbial communities. Soil Biol Biochem 33:1713–1722

Gu B, Schmitt J, Chen Z, Liang L, McCarthy JF (1994) Adsorption and desorption of natural organic matter on iron oxide: mechanisms and models. Environ Sci Technol 28:38–46

Guan X-H, Shang C, Chen G-H (2006) ATR-FTIR investigation of the role of phenolic groups in the interaction of some NOM model compounds with aluminum oxide. Chemosphere 65:2074–2081

Guggenberger G, Kaiser K (2003) Dissolved organic matter in soil: challenging the paradigm of sorptive preservation. Geoderma 113:293–310

Gunderson P, Emmett BA, Kjønaas OJ, Koopmans CJ, Tietema A (1998) Impact of nitrogen deposition on nitrogen cycling in forests: a synthesis of NITREX data. For Ecol Manage 101:37–55

Güsewell S, Gessner MO (2009) N:P ratios influence litter decomposition and colonization by fungi and bacteria in microcosms. Funct Ecol 23:211–219

Heckman K, Rasmussen C, Chorover J, Vasquez Ortega A, Gao X (2011) Changes in water extractable organic matter during incubation of forest floor material in the presence of quartz, goethite and gibbsite surfaces. Geochim Cosmochim Acta 75:4295–4309

Hunt JF, Ohno T, He Z, Honeycutt CW, Dail DB (2007) Inhibition of phosphorus sorption to goethite, gibbsite and kaolin by fresh and decomposed organic matter. Biol Fertil Soils 44:277–288

Jandl R, Sollins P (1997) Water-extractable soil carbon in relation to the belowground carbon cycle. Biol Fert Soils 25:196–201

Journey JS, Anderson RM, Essington ME (2010) The adsorption of 2-ketogluconate by goethite. Soil Sci Soc Am J 74:1119–1128

Kaiser K, Mikutta R, Guggenberger G (2007) Increased stability of organic matter sorbed to ferrihydrite and goethite on aging. Soil Sci Soc Am J 71:711–719

Kalbitz K, Solinger S, Park J-H, Michalzik B, Matzner E (2000) Controls on the dynamics of dissolved organic matter in soils: a review. Soil Sci 165:277–304

Kalbitz K, Schmerwitz J, Schwesig D, Matzner E (2003) Biodegradation of soil-derived dissolved organic matter as related to its properties. Geoderma 113:273–291

Keil RG, Montluçon DB, Prahl FG, Hedges JI (1994) Sorptive preservation of labile organic matter in marine sediments. Nature 370:549–552

Kögel-Knabner I, Guggenberger G, Kleber M, Kandler E, Kalbitz K, Scheu S, Eusterhues K, Leinweber P (2008) Organo-mineral associations in temperate soils: Integrating biology, mineralogy, and organic matter chemistry. J Plant Nutr Soil Sci 171:61–82

Marschner B, Kalbitz K (2003) Controls of bioavailability and biodegradability of dissolved organic matter in soils. Geoderma 113:211–235

Mccune B, Mefford MJ (2006) PC-ORD. Multivariate Analysis of Ecological Data. Version 5 MJM software design. Gleneden Beach, Oregon, USA

McDowell WH (2002) Dissolved organic matter in soils: future directions and unanswered questions. Geoderma 113:179–186

McKnight DM, Bencala KE, Zeliweger GW, Aiken GR, Feder GL, Thorn KA (1992) Sorption of dissolved organic carbon by hydrous aluminum and iron oxides occurring at the confluence of Deer Creek with the Snake River, Summit County. Colorado. Environ. Sci. Technol. 26:1388–1396

Metting FB (1993) Structure and physiological ecology of soil microbial communities. In: Metting FB (ed) Soil microbial ecology: application in agricultural and environmental management. Marcel Dekker, New York, pp 3–24

Mikutta R, Kleber M, Torn MS, Jahn R (2006) Stabilization of soil organic matter: association with minerals or chemical recalcitrance? Biogeochemistry 77:25–56

Mikutta R, Zhang U, Chorover J, Haumaier L, Kalbitz K (2011) Stabilization of extracellular polymeric substances by adsorption versus co-precipitation with hydroxyl-aluminum species. Geochim Cosmochim Acta 75:3135–3154

Molis E, Barrès O, Marchand H, Sauzéat E, Humbert B, Thomas F (2000) Initial steps of ligand-promoted dissolution of gibbsite. Colloid Surface A 163:283–292

Mv Lützow, Kögel-Knabner I, Ekschmitt K, Matzner E, Guggenberger G, Marschner B, Flessa H (2006) Stabilization of organic matter in temperate soils: mechanisms and their relevance under different soil conditions: a review. Eur J Soil Sci 57:426–445

Nierop KGJ, Jansen B, Verstraten JM (2002) Dissolved organic matter, aluminum and iron interactions: precipitation induced by metal/carbon ratio, pH and competition. Sci Total Environ 300:201–211

Ognalaga M, Frossard E, Thomas F (1994) Glucose-1-phosphate and myo-inositol hexaphosphate adsorption mechanisms on goethite. Soil Sci Soc Am J 58:332–337

Ohno T, Chorover J, Omoike A, Hunt J (2007) Molecular weight and humification index as predictors of adsorption for plant- and manure-derived dissolved organic matter to goethite. Eur J Soil Sci 58:125–132

Omoike A, Chorover J (2006) Adsorption to goethite of extracellular polymeric substances from *Bacillus subtilis*. Geochim Cosmochim Acta 70:827–838

Parfitt RL, Fraser AR, Farmer VC (1977) Adsorption on hydrous oxides. III. Fulvic acid and humic acid on goethite, gibbsite and imogolite. Eur J Soil Sci 28:289–296

Paul EA, Clark FE (1996) Soil microbiology and biochemistry. Academic Press, San Diego

Rasmussen C, Southard RJ, Horwath WR (2006) Mineral control of organic carbon mineralization in a range of temperate conifer forests. Glob Change Biol 12:834–847

Rousk J, Bååth E, Brookes PC, Lauber CL, Lozupone C, Caporaso JG, Knight R, Fierer N (2010) Soil bacterial and fungal communities across a pH gradient in an arable soil. ISME J 4:1340–135

Saggar S, Parfitt RL, Salt G, Skinner MF (1998) Carbon and phosphorus transformations during decomposition of pine forest floor with different phosphorus status. Biol Fertil Soils 27:197–204

Scheel T, Dörfler C, Kalbitz K (2007) Precipitation of dissolved organic matter by aluminum stabilizes carbon in acidic forest soils. Soil Sci Soc Am J 71:64–74

Schmidt MWI, Torn MS, Abiven S, Dittmar T, Guggenberger G, Janssens IA, Kleber M, Kogel-Knabner I, Lehmann J, Manning DAC, Nannipieri P, Rasse DP, Weiner S, Trumbore SE (2011) Persistence of soil organic matter as an ecosystem property. Nature 478:49–56

Schneider MPW, Scheel T, Mikutta R, van Hees P, Kaiser K, Kalbitz K (2010) Sorptive stabilization of organic matter by amorphous Al hydroxide 74:1606–1619

Schnittler M, Stephenson SL (2000) Myxomycete biodiversity in four different forest types in Costa Rica. Mycologia 92:626–637

Schutter M, Dick R (2001) Shifts in substrate utilization potential and structure of soil microbial communities in response to carbon substrates. Soil Biol Biochem 33:1481–1491

Schwesig D, Kalbitz K, Matzner E (2003) Effects of aluminium on the mineralization of dissolved organic carbon derived from forest floors. Eur J Soil Sci 54:311–322

Shang C, Caldwell DE, Stewart JWB, Tiessen H, Huang PM (1996) Bioavailability of organic and inorganic phosphates adsorbed on short-range ordered aluminium precipitate. Microb Ecol 31:29–39

Six J, Conant RT, Paul EA, Paustian K (2002) Stabilization mechanisms of soil organic matter: Implications for C-saturation of soils. Plant Soil 241:155–176

Six J, Frey SD, Thiet RK, Batten KM (2006) Bacterial and fungal contributions to carbon sequestration in agroecosystems. Soil Sci Soc Am J 70:555–569

Smith VH (2002) Effects of resource supply ratios on the structure and function of microbial communities. Antonie Van Leeuwenhoek 81:99–106

Sollins P, Homann P, Caldwell BA (1996) Stabilization and destabilization of soil organic matter: mechanisms and controls. Geoderma 74:65–105

Stevenson FJ (1994) Humus chemistry: genesis, composition, reactions, 2nd edn. Wiley, New York

Stevenson FJ, Cole MA (1999) Cycles of soil: carbon, nitrogen, phosphorus, sulfur, micronutrients, 2nd edn. Wiley, New York

Stuanes AO, Kjønass OJ (1998) Soil solution chemistry during four years of NH_4NO_3 addition to a forested catchment at Gårdsjön, Sweden. For Ecol Manage 101:215–226

Tate RL III (1987) Soil organic matter: biological and ecological effects. Wiley, New York

van der Heijden MGA, Bardgett RD, van Straalen NM (2008) The unseen majority: soil microbes as drivers of plant diversity and productivity in terrestrial ecosystems. Ecol Lett 11:296–310

Wagai R, Sollins P (2002) Biodegradation and regeneration of water-soluble organic carbon in a forest soil: leaching column study. Biol Fert Soils 35:18–26

Walker BH (1992) Biodiversity and ecological redundancy. Conserv Biol 6:18–23

Wertz S, Degrange V, Prosser JI, Poly F, Commeaux C, Freitag T, Guillaumaud N, Le Roux X (2006) Maintenance of soil functioning following erosion of microbial diversity. Environ Microbiol 8:2162–2169

Wickings K, Grandy AS, Reed S, Cleveland C (2011) Management intensity alters decomposition via biological pathways. Biogeochemistry 104:365–379

Wood M (1995) A mechanism of aluminum toxicity to soil bacteria and possible ecological implications. Plant Soil 171:63–69

Wright CJ, Coleman DC (2000) Cross-site comparison of soil microbial biomass, soil nutrient status, and nematode trophic groups. Pedobiologia 44:2–23

Zech W, Guggenberger G (1996) Organic matter dynamics in forest soils of temperate and tropical ecosystems. In: Piccolo A (ed) Humic substances in terrestrial ecosystems. Elsevier, Amsterdam, pp 101–170

Zibilske LM (1994) Carbon mineralization. In: Weaver RW, Angle S, Bottomley P (eds) Methods of soil analysis part 2: microbiological and biochemical properties. Soil Science Society of America, Inc. Madison, pp 835–864

Zsolnay A (1996) Dissoved humus in soil waters. In: Piccolo A (ed) Humic substances in terrestrial ecosystems. Elsevier, Amsterdam, pp 225–264